Yogita Kalra

FINAL THESIS (NU)

PHD

Document Details

Submission ID
trn:oid:::27535:140651753

Submission Date
May 27, 2026, 4:24 PM GMT+5:30

Download Date
May 27, 2026, 4:36 PM GMT+5:30

File Name
FINAL THESIS (NU).docx

File Size
1.5 MB

42 Pages

11,170 Words

63,947 Characters

5% Overall Similarity

The combined total of all matches, including overlapping sources, for each database.

Filtered from the Report

- Bibliography
- Small Matches (less than 10 words)

Match Groups

33 Not Cited or Quoted 5%
Matches with neither in-text citation nor quotation marks

0 Missing Quotations 0%
Matches that are still very similar to source material

0 Missing Citation 0%
Matches that have quotation marks, but no in-text citation

0 Cited and Quoted 0%
Matches with in-text citation present, but no quotation marks

Top Sources

3% Internet sources
2% Publications
3% Submitted works (Student Papers)

Integrity Flags

0 Integrity Flags for Review

Our system's algorithms look deeply at a document for any inconsistencies that would set it apart from a normal submission. If we notice something strange, we flag it for you to review.

A Flag is not necessarily an indicator of a problem. However, we'd recommend you focus your attention there for further review.

Match Groups

- **33** Not Cited or Quoted 5%
  Matches with neither in-text citation nor quotation marks
- **0** Missing Quotations 0%
  Matches that are still very similar to source material
- **0** Missing Citation 0%
  Matches that have quotation marks, but no in-text citation
- **0** Cited and Quoted 0%
  Matches with in-text citation present, but no quotation marks

Top Sources

3% Internet sources
2% Publications
3% Submitted works (Student Papers)

Top Sources

The sources with the highest number of matches within the submission. Overlapping sources will not be displayed.

1	Student papers	Delhi Technological University on 2026-05-26 <1%
2	Internet	dspace.dtu.ac.in:8080 <1%
3	Internet	dspace.christcollegeijk.edu.in:8080 <1%
4	Internet	thesis.lib.ncku.edu.tw <1%
5	Student papers	Delhi Technological University on 2020-06-01 <1%
6	Student papers	Delhi Technological University on 2026-04-13 <1%
7	Student papers	Delhi Technological University on 2026-05-18 <1%
8	Internet	www.preprints.org <1%
9	Internet	discol.umk.edu.my <1%
10	Internet	files01.core.ac.uk <1%

11 Internet
acikbilim.yok.gov.tr <1%

12 Student papers
Higher Education Commission Pakistan on 2019-04-18 <1%

13 Student papers
Middlesex University on 2026-01-01 <1%

14 Student papers
National University of Ireland, Galway on 2020-04-03 <1%

15 Internet
researchrepository.murdoch.edu.au <1%

16 Internet
www.ioa.org.uk <1%

17 Student papers
Delhi Technological University on 2026-05-25 <1%

18 Publication
Holt, R.S.. "Magnetic compton scattering with circularly polarised synchrotron r... <1%

19 Publication
Tadahiro Ohmi. "Ultraclean Technology Handbook - Ultrapure Water", CRC Press, ... <1%

20 Student papers
University of Sydney on 2025-11-06 <1%

21 Internet
www.frontiersin.org <1%

22 Internet
www.mdpi.com <1%

23 Student papers
DU Faculty Members on 2026-05-24 <1%

24 Student papers
Indian Institute of Technology, Madras on 2026-05-20 <1%

25 Student papers

Monash University on 2025-11-10 <1%

26 Publication

Yonghui Tan, Yunping Qi, Xinmiao Ding, Wenqing Guan, Bing Luo. "Tunable conti... <1%

27 Internet

ethesisarchive.library.tu.ac.th <1%

28 Internet

www.metabunk.org <1%

DESIGN AND ANALYSIS OF TEMPERATURE TUNABLE CHIRAL METASURFACE

A Thesis submitted
in partial fulfilment of the requirements for the award of the degree of

MASTER OF SCIENCE
in
PHYSICS

Submitted by

NAMAN UPADHYAY
(Roll No. 24/MSCPHY/10)

Under the supervision of

Dr. Yogita Kalra
Associate Professor, Department of Applied Physics
Delhi Technological University

DEPARTMENT OF APPLIED PHYSICS
DELHI TECHNOLOGICAL UNIVERSITY
(Formerly Delhi College of Engineering)
Shahbad Daulatpur, Main Bawana Road, Delhi-110042

DELHI TECHNOLOGICAL UNIVERSITY
(Formerly Delhi College of Engineering)
Shahbad Daulatpur, Main Bawana Road, Delhi-110042

CANDIDATE'S DECLARATION

I, Naman, Roll No. 24/MSCPHY/10, student of M.Sc. Physics, hereby declare that the dissertation titled "Design and Analysis of Temperature Tunable Chiral Metasurface", submitted to the Department of Applied Physics, Delhi Technological University, in partial fulfilment of the requirements for the award of the degree of Master of Science in Physics, is an authentic record of my own work carried out under the supervision of Dr. Yogita Kalra.

The matter presented in this dissertation has not been submitted by me for the award of any other degree or diploma of this University or any other institution. All sources used in the dissertation have been acknowledged through appropriate citation.

Place: Delhi (Naman)
Date:29/5/26

DELHI TECHNOLOGICAL UNIVERSITY
(Formerly Delhi College of Engineering)
Shahbad Daulatpur, Main Bawana Road, Delhi-110042

CERTIFICATE BY THE SUPERVISOR

This is to certify that the dissertation titled "Design and Analysis of Temperature Tunable Chiral Metasurface" submitted by Naman (Roll No. 24/MSCPHY/10) to the Department of Applied Physics, Delhi Technological University, in partial fulfilment of the requirements for the award of the degree of Master of Science in Physics, is a record of bona fide research work carried out by him under my supervision.

To the best of my knowledge, the contents of this dissertation, in full or in parts, have not been submitted to any other institute or university for the award of any degree or diploma.

Place: Delhi
Date:29/5/2026

Dr. Yogita Kalra
Associate Professor
Department of Applied Physics
Delhi Technological University

ACKNOWLEDGEMENTS

I am sincerely grateful to my supervisor, Dr. Yogita Kalra, Associate Professor, Department of Applied Physics, Delhi Technological University, for her guidance, academic support, and careful supervision throughout this dissertation work. Her suggestions helped me understand the physical basis of metasurface design and improve the interpretation of the simulated results.

I would also like to thank the PhD Scholar Ms. Vishakha Sharma for helping me in the learning and simulation phases of this work. Her inputs were helpful to understand how chiral metasurface structures are analyzed in computational studies.

I am also thankful to the faculty members of the Department of Applied Physics, Delhi Technological University, for providing the required academic environment suited for research. I also want to thank my friends namely Mr. Kislay Kumar, Mr. Vibhu Xaxa for their support during the preparation of this dissertation.

Naman
(24/MSCPHY/10)

ABSTRACT

Metasurfaces are defined as two-dimensional electromagnetic structures composed of subwavelength unit cells. Their optical response depends not only on the bulk material properties but also on geometry, choice of material and near-field coupling. In this dissertation, the design and simulation-based analysis of a temperature tunable chiral metasurface in near infrared region is presented. The proposed unit cell is composed of a gold ground plane, a PTFE dielectric layer, a thin layer of vanadium dioxide, and a gold top resonator with an asymmetric hollow crescent geometry. The geometry is designed to generate varying absorption responses for incident radiation with left and right circular polarization.

The work is about circular dichroism and polarization-selective absorption. The optical response of the periodic metasurface was obtained over the wavelength range of 1100 nm to 2500 nm by modeling it using the CST Studio Suite. A metallic ground plane inhibits transmission, and thus the absorptance is mainly evaluated through the reflection response. Thermal reconfigurability can be achieved by including vanadium dioxide as VO_2 undergoes an insulator-to-metal transition at about 68 °C. Such a transition alters the conductivity and optical permittivity of the active layer, which in turn changes the field confinement, the impedance matching and the resonance damping.

The metasurface exhibits a strong chiroptical response with a maximum circular dichroism of about 0.829 near the wavelength of 1304 nm at 25 °C. Absorption for left circularly polarized radiation is about 0.976 and for right circularly polarized radiation it is close to 0.275. The absorption values of the two circular polarization states become closer and the peak circular dichroism at 100 °C is reduced to about 0.481 around 1485 nm. This result demonstrates that the metallic phase of VO_2 decreases the asymmetry of the resonance response through enhanced damping and alteration of the effective impedance of the cavity.

A parametric analysis was also carried out for the VO_2 layer thickness and incidence angle. The analysis shows that the thinner VO_2 layer results in stronger spectral contrast, while increasing the VO_2 thickness results in shifting and broadening of the resonance. The angular study reveals that the chiral response increases for larger oblique incidence angles in the simulated range. Combined, these results suggest that a VO_2-based chiral metasurface is a promising route towards active polarization control, infrared modulation, adaptive absorbers and sensing platforms where thermal tuning is advantageous.

TABLE OF CONTENTS

CANDIDATE'S DECLARATION ii
CERTIFICATE BY THE SUPERVISOR iii
ACKNOWLEDGEMENTS iv
ABSTRACT v
TABLE OF CONTENTS vi
LIST OF TABLES vii
LIST OF FIGURES viii
LIST OF SYMBOLS, ABBREVIATIONS AND NOMENCLATURE ix
CHAPTER 1: INTRODUCTION 1
1.1 Background 1
1.2 Motivation 2
1.3 Problem Statement 3
1.4 Research Gap 3
1.5 Objectives 3
1.6 Scope of the Work 4
1.7 Organisation of the Dissertation 4
CHAPTER 2: THEORETICAL BACKGROUND AND LITERATURE REVIEW 6
2.1 Metamaterials, Metasurfaces and Meta-atoms 6
2.2 Circular Polarization and Circular Dichroism 7
2.3 Absorptance, Reflectance and Transmission 8
2.4 Impedance Matching and Resonant Loss 8
2.5 Quality Factor and Resonance Selectivity 9
2.6 Fano Resonance and Interference in Metasurfaces 10
2.7 Vanadium Dioxide as a Phase-Transition Material 10
2.8 Passive and Active Chiral Metasurfaces 10
2.9 Intrinsic and Extrinsic Chirality 11
2.10 Why Absorption-Based CD Matters 11
2.11 Review of Relevant Chiral Metasurface Studies 12
2.12Position of the Present Work 13
CHAPTER 3: PROPOSED METASURFACE DESIGN AND SIMULATION METHODOLOGY 14
3.1 Design Philosophy 14
3.2 Unit Cell Geometry 14

3.3 Material Platform 15
3.4 Material Assumptions in Numerical Modelling 16
3.5 Numerical Validation Strategy 17
3.6 Reason for Using Two Temperature States 17
3.7 Circular Polarization Excitation 17
3.8 Boundary Conditions and Solver Setup 18
3.9 Temperature States 18
CHAPTER 4: RESULTS AND DISCUSSION 20
4.1 Overview of Temperature-Dependent Response 20
4.2 Circular Dichroism at 25 °C 21
4.3 Polarization-Dependent Absorption at 25 °C 22
4.4 Circular Dichroism at 100 °C 23
4.5 Polarization-Dependent Absorption at 100 °C 24
4.6 Reading the Two-Peak CD Profile 25
4.7 Spectral Shift After Thermal Transition 25
4.8 Modulation Depth of Circular Dichroism 25
4.9 Interpretation of Absorption Balance 26
4.10 Quantitative Comparison Between Temperature States 26
4.11 Physical Interpretation of the Temperature Response 27
4.12 Comparison With Reported Metasurface Studies 28
CHAPTER 5: PARAMETRIC ANALYSIS 29
5.1 Purpose of Parametric Evaluation 29
5.2 Effect of VO_2 Layer Thickness 30
5.3 Interpretation Through Loss and Field Overlap 31
5.4 Design Guidelines From the Thickness Study 31
5.5 Suggested Additional Parameters for Optimization 32
5.6 Angular Stability as a Device Metric 32
5.7 Thickness and Temperature Coupling 32
5.8 Angular Dependence of the Chiral Response 33
5.9 Angular Response and Practical Design 34
CHAPTER 6: PHYSICS-BASED DISCUSSION AND DESIGN IMPLICATIONS 35
6.1 Role of the Hollow Crescent Geometry 35

6.2 Role of the Gold Ground Plane 35
6.3 Role of PTFE Dielectric Spacer 36
6.4 Role of VO_2 Placement 36
6.5 Why Circular Dichroism Falls at High Temperature 36
6.6Experimental Characterization Route 37
6.7 Connection to Biosensing and Molecular Detection 38
6.8 Limitations of the Present Study 38
CHAPTER 7: CONCLUSION, FUTURE SCOPE AND SOCIAL IMPACT 40
7.1 Conclusion 40
7.2 Major Findings 41
7.3 Future Scope 41
7.4 Possible Applications 42
7.5 Final Remarks 43
APPENDIX A: SUPPLEMENTARY SIMULATION RELATIONS 44
A.1 Absorption From Scattering Parameters 44

LIST OF TABLES

3.1 Main structural parameters used for the proposed unit cell. 15
3.2 Simulation settings used in the supplied study. 18
4.1 Key simulated chiroptical results at 25 °C and 100 °C. 26
4.2 Comparison with selected studies from the supplied reference collection. ... 28
5.1 Qualitative effect of increasing VO_2 thickness based on the supplied CD spectra. 31
B.1 Source register for figures used in this dissertation. 45

LIST OF FIGURES

2.1 Schematic hierarchy from one-dimensional structures to two-dimensional metasurfaces and three-dimensional metamaterials. Source: uploaded draft figure from NAMAN final msc thesis.docx. 6

3.1 Top and side views of the proposed hollow crescent chiral metasurface unit cell. Source: uploaded draft figure from NAMAN final msc thesis.docx. 15

4.1 Circular dichroism spectrum of the optimized structure at 25 °C. Source: present CST simulation graph supplied in the Naman Plots archive..... 21

4.2 Absorption spectra for LCP and RCP radiation at 25 °C. Source: present CST simulation graph supplied in the Naman Plots archive. 22

4.3 Circular dichroism spectrum of the optimized structure at 100 °C. Source: present CST simulation graph supplied in the Naman Plots archive..... 23

4.4 Absorption spectra for LCP and RCP radiation at 100 °C. Source: present CST simulation graph supplied in the Naman Plots archive. 24

5.1 Circular dichroism spectra at 25 °C for different VO_2 layer thicknesses. Source: present CST simulation graph supplied in the Naman Plots archive. 30

5.2 Circular dichroism spectra at 25 °C for different incidence angles. Source: present CST simulation graph supplied in the Naman Plots archive. 33

LIST OF SYMBOLS, ABBREVIATIONS AND NOMENCLATURE

Symbol or abbreviation	Meaning
A	Absorptance of the metasurface
A_L	Absorptance for left circularly polarized incident radiation
A_R	Absorptance for right circularly polarized incident radiation
CD	Circular dichroism
CPL	Circularly polarized light
CST	Computer Simulation Technology Studio Suite
FIT	Finite integration technique
FEM	Finite element method
FWHM	Full width at half maximum
LCP	Left circularly polarized radiation
RCP	Right circularly polarized radiation
R	Reflectance
T	Transmittance
S_{11}	Reflection scattering parameter
S_{21}	Transmission scattering parameter
p_x, p_y	Unit cell periodicity along x and y directions
h_1	Thickness of bottom gold layer
h_2	Thickness of PTFE dielectric spacer
h_3	Thickness of VO_2 active layer
h_4	Thickness of top gold resonator
θ	Incidence angle
VO_2	Vanadium dioxide
PTFE	Polytetrafluoroethylene

CHAPTER 1
INTRODUCTION

1.1 Background

Metamaterials and metasurfaces form a class of engineered electromagnetic media whose response is shaped by subwavelength structuring. A conventional material responds to incident radiation through its composition and microscopic electronic structure. A metasurface, by contrast, adds another design layer. It allows the researcher to change the phase, amplitude, absorption, and polarization response of light through the geometry of patterned resonators. This distinction is central to the present work, because the proposed response does not follow from gold, PTFE, or VO_2 in isolation. It emerges from the way these materials are arranged in a chiral, resonant, and thermally active unit cell.

The shift from bulk metamaterials to metasurfaces has a practical origin. Three-dimensional metamaterials often require thick, multilayer structures, while a metasurface offers wave manipulation in a planar and fabrication-friendly form. The physical idea is the same. Subwavelength building blocks act as meta-atoms and their collective response leads to optical properties not typically found in natural media. In this area, the negative index of refraction, large absorption, optical activity and polarization conversion have been extensively discussed [5]. The concept of an absorber presented by Landy et al. (2008) is especially relevant here, and it shows how independent electric and magnetic responses can lead to strong absorption when both reflection and transmission are suppressed.

Chiral metasurfaces are an important, but narrower, area of this field.Natural chiral media are typically weakly circularly dichroic, which reduces the potential for direct optical detection in many applications (Barron 2009; Valev et al. 2013). The subwavelength geometry of artificial chiral metasurfaces induces strong local field enhancement and asymmetric current distributions [9], which overcome this limitation. Thus these structures are found in studies of polarization optics, chiral sensing, infrared detection and optical modulation [10].

This dissertation studies a thermally tunable chiral metasurface based on vanadium dioxide. The importance of VO_2 stems from the fact that its optical constants vary greatly near the insulator-to-metal transition temperature [11]. In many reported systems, the chiral response is fixed after the fabrication [13]. This fixed response is fine for static filters or absorbers, but not so good for adaptive devices. The inclusion of VO_2 provides a path for active control. A change in temperature changes the conductivity which changes the resonance condition, field localization and absorption contrast between LCP and RCP waves.

The chosen design uses a gold ground plane, a PTFE spacer, a thin VO_2 layer, and a gold top resonator in the form of asymmetric hollow crescent cavities. The ground plane suppresses transmission. The spacer and resonator create a cavity-like environment. The crescent geometry breaks symmetry and produces unequal coupling to opposite circular polarization states. The VO_2 layer provides thermal modulation. Taken together, these choices define the scientific question of the

dissertation: how does the thermally driven phase transition of VO_2 reshape circular dichroism and polarization-selective absorption in a chiral metasurface?

1.2 Motivation

The motivation behind this work is a tension in current metasurface research. Strong chiral response typically requires sharp resonance and asymmetric near-field coupling. Active tunability often introduces loss, damping and fabrication complexity. The design should balance these effects giving strong circular dichroism at low temperature and measurable thermal switching at high temperature. It should be chiral and yet permit the active layer to influence the cavity response.

Research on VO_2-based metasurfaces explains the importance of this balance. Zhao et al. (2023) described a large switchable asymmetric transmission and circular conversion dichroism in a VO_2 based metasurface with the chiral effect switched over a wide range during the phase transition. Their work shows the promise of VO_2 as a useful active material for dynamic polarization control. And yet this dissertation is not a reiteration of that geometry. The proposed structure consists of a near-infrared multilayer absorber backed by gold and a PTFE platform with crescent cavity. Absorption-based circular dichroism is considered rather than transmission-based asymmetric propagation.

Meanwhile, studies on chiral metasurface biosensors show the sensing information can be obtained from the magnitude and spectral position of circular dichroism. Sharma, Kalra, and Sinha (2025) have designed a triple-band perovskite chiral metasurface with circular dichroism in the visible, near-infrared and mid-infrared regions for biosensing. This work demonstrates how resonant cavities and asymmetric field distributions enable label-free detection. The current dissertation is based on the same general idea of utilizing CD as a measurable optical signature, but in this case the active component is temperature instead of analyte refractive index.

1.3 Problem Statement

Most passive chiral metasurfaces exhibit a fixed electromagnetic response after fabrication. This limits their use in adaptive devices where polarization response needs to be modified without changing the physical geometry. A second issue arises from the fact that strong absorption and strong chiral contrast do not always occur together. A structure might absorb well while showing weak difference between LCP and RCP radiation. Another structure might show high CD but weak total absorption. For temperature-responsive metasurfaces, additional constraints appear because the active layer modifies both resonance and loss.

The problem addressed in this dissertation is the design and analysis of a thermally tunable chiral metasurface that combines high polarization-selective absorption with a measurable change in circular dichroism between room temperature and elevated temperature. The work asks whether a thin VO_2 layer embedded in an asymmetric hollow crescent resonator geometry is able to tune the CD response in the near-infrared region while retaining a clear contrast between LCP and RCP absorption.

1.4 Research Gap

The literature shows strong progress in chiral metasurfaces, absorbers, and phase-change materials. Still, three gaps motivate this dissertation. First, many high-CD metasurfaces are passive. Once fabricated, their optical response is fixed unless the operating environment changes. Second, some active structures focus on terahertz transmission, while near-infrared absorption-based chiral tuning remains a useful direction for compact photonic devices. Third, the physical interpretation of VO_2-assisted chirality requires careful discussion because the phase transition changes conductivity, permittivity, damping, and impedance at the same time.

The present work addresses these gaps by studying a gold-PTFE-VO_2-gold metasurface in which the active layer lies inside a resonant chiral cavity. It does not claim to solve every limitation of tunable chiral metasurfaces. Rather, it evaluates a specific design route and interprets the simulated results using absorption theory, circular dichroism, resonance confinement, and thermal phase transition physics.

17

1.5 Objectives

The objectives of the dissertation are as follows.

1. To design a multilayer chiral metasurface using gold, PTFE, and VO_2 for operation in the near-infrared spectral region.
2. To analyse the absorption response for LCP and RCP incident radiation using CST Studio Suite.
3. To calculate the circular dichroism response at 25 °C and 100 °C.
4. To examine how the VO_2 phase transition modifies resonance confinement, impedance matching, and polarization selectivity.
5. To evaluate the influence of VO_2 layer thickness and incidence angle on the CD spectrum.
6. To situate the obtained results within the broader literature on chiral metasurfaces, absorbers, and VO_2-based active photonic structures.

1.6 Scope of the Work

This dissertation is limited to theoretical design and full-wave electromagnetic simulation. The study does not include fabrication, material deposition, thermal cycling experiments, or optical characterization by laboratory instruments. The geometric model and spectral results are based on CST Studio Suite simulations supplied in the project files. The wavelength range considered is 1100 nm to 2500 nm. The discussion is framed around circular dichroism, absorption, and temperature-dependent tuning of VO_2.

The scope is still broad enough to support a physics-based analysis. The dissertation discusses the relation between scattering parameters and absorptance, the role of a ground plane, resonance linewidth, field confinement, and thermal phase transition. It also places the proposed design in relation to reported metasurface studies that use VO_2, chiral resonators, and absorber architectures.

1.7 Organization of the Dissertation

The dissertation is built around the scientific development of the work. Chapter 1 outlines the motivation, problem statement, research gap, objectives and scope. In Chapter 2 the theoretical background needed to read the results is developed, including absorption, scattering parameters, circular dichroism, VO2 phase transition and relevant literature. Chapter 3 introduces the proposed unit cell, the material platform, the simulation method and the data-processing approach. Chapter 4 presents the main temperature dependent results and the change of circular dichroism between 25 °C and 100 °C is interpreted. Chapter 5 is devoted to the parametric analysis of the VO_2 thickness and of the incidence angle. Chapter 6 extends the discussion of the design and its implications to a wider physics-based view. The work is concluded in Chapter 7 and directions for future work are given.

CHAPTER 2
THEORETICAL BACKGROUND AND LITERATURE REVIEW

2.1 Metamaterials, Metasurfaces and Meta-atoms

The term metamaterial refers to an artificial medium whose electromagnetic response arises from designed structure. In many cases, the unit cell is much smaller than the wavelength of the incident radiation. This subwavelength condition allows the array to be treated as an effective medium in a limited spectral region [3]. A metasurface is the planar version of this idea. Instead of relying on a thick three-dimensional arrangement, it uses patterned elements on or within a thin layer.

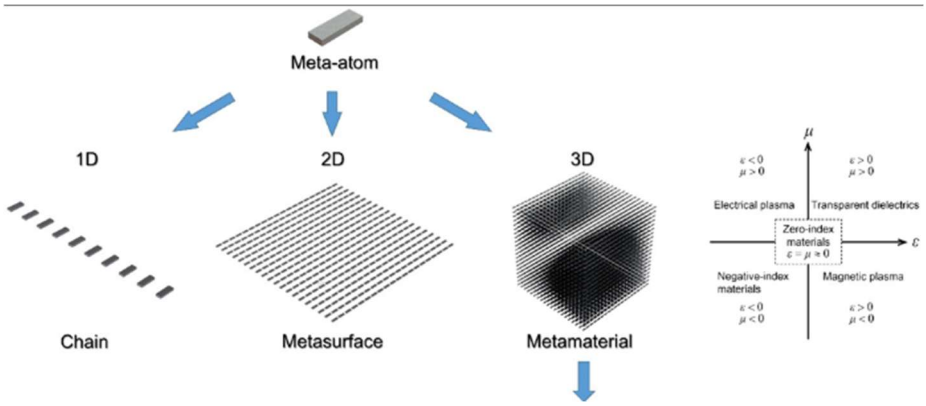

Figure 2.1: Schematic hierarchy from one-dimensional structures to two-dimensional metasurfaces and three-dimensional metamaterials

The concept of a meta-atom is useful but should not be taken too literally. A natural atom responds through electronic energy levels and quantum transitions. A meta-atom responds through resonant currents, capacitive gaps, inductive loops, and near-field coupling. The analogy helps explain why periodic arrays produce a collective optical response. It also clarifies why small changes in geometry strongly affect the resonance wavelength.

Negative refraction is one of the early examples of an unusual response associated with metamaterials. If the effective permittivity and permeability are both negative, then the phase velocity and the energy flow are not related in the usual way in that medium. Negative refraction is not the immediate subject of this dissertation, but it does illustrate the broader principle behind the field: geometry modifies electromagnetic response. A different observable, namely the circular dichroism, reveals the same principle in the proposed chiral metasurface.

Metasurfaces are most suitable for optical and infrared devices due to their thickness being less than the free space wavelength. This small size is important for combining with sensors, photonic chips, detectors and adaptive optical elements [5]. At the same time the plane shaped geometry puts limitations. Some strong chiral effects require broken symmetry along the propagation direction or carefully designed in-plane asymmetry. The present design uses asymmetric hollow crescent cavities to create unequal response to opposite circular polarization states.

2.2 Circular Polarization and Circular Dichroism

An electromagnetic wave is circularly polarized when the electric field vector rotates as the wave propagates. The two handed states are left circular polarization and right circular polarization. A chiral structure interacts differently with these two states. The measurable difference in absorption is called circular dichroism.

For an absorption-based chiral metasurface, CD is defined as

$$\mathrm{CD} = A_L - A_R \qquad 1$$

where A_L is the absorptance for left circularly polarized radiation and A_R is the absorptance for right circularly polarized radiation. Some studies define CD using transmission or reflection contrast, depending on device geometry and measurement mode. In a ground-plane-backed absorber, transmission is suppressed, so an absorption-based definition is appropriate.

The physical origin of CD in metasurfaces lies in asymmetric coupling. If LCP and RCP waves induce the same current pattern with the same amplitude and phase, the CD value is close to zero. If one handedness excites a strongly confined resonance while the other couples weakly, the CD value increases. The difference arises from the geometry of the resonator, the orientation of the field, and the distribution of induced surface currents.

The molecular CD can be weak in nature because of the small interaction volume and the low optical chirality of the field. This interaction is made possible by plasmonic and dielectric metasurfaces which localize fields in nanoscale regions (Valev et al. 2013; Warning et al. 2021). This improvement in sensing is useful for detecting small refractive-index changes or molecular symmetry. The same development of polarization devices helps in the development of selective absorbers, polarizers and filters.

The important point for the present design is the existence of CD and not only. It is the control of CD by means of temperature. A high CD at 25 °C indicates a strong asymmetric absorption. The CD at 100 °C is lower, meaning that the VO$_2$ phase transition changes the coupling. The transition between these two states is the primary confirmation of thermal tuning.

2.3 Absorptance, Reflectance and Transmission

When electromagnetic waves fall on a metasurface, the energy conservation gives

$$A(\lambda) + R(\lambda) + T(\lambda) = 1, \qquad 2$$

where A is absorptance, R is reflectance, and T is transmittance. In simulations based on scattering parameters,

$$R(\lambda) = |S_{11}(\lambda)|^2,$$
$$T(\lambda) = |S_{21}(\lambda)|^2.$$

Substitution into Eq. [eq:energy] gives

$$A(\lambda) = 1 - |S_{11}(\lambda)|^2 - |S_{21}(\lambda)|^2. \qquad 3$$

In the proposed structure, the bottom gold layer acts as a ground plane. It strongly suppresses transmission through the structure, so $T(\lambda)$ is approximately zero. The absorptance is then written as

$$A(\lambda) \simeq 1 - |S_{11}(\lambda)|^2. \quad 4$$

This relationship is key because it shows why low reflection suggests high absorption in the present geometry. The structure couple's incident energy into localized modes, releasing that energy through metallic, dielectric, and active-material losses, producing a resonance peak in absorption. This interpretation can be defined on the basis of the literature on absorbers. Landy et al. (2008) showed that near-unity absorption requires suppression of both transmission and reflection, with impedance matching to free space being critical. The present metasurface is based on the same physical logic, but adds polarization selectivity and thermal tunability.

2.4 Impedance Matching and Resonant Loss

The metasurface absorber works well when the incident waves enter the resonant structure rather than being strongly reflected. The condition is often stated in terms of effective impedance. For a structure with effective ε and permeability $\mu$the averaged impedance is conventionally written as

$$Z_{\text{eff}} = \sqrt{\frac{\mu_{\text{eff}}}{\epsilon_{\text{eff}}}}. \quad 5$$

When Z_{eff} approaches the free-space impedance, reflection decreases [3]. The energy that enters the metasurface is then dissipated through material loss and resonant current flow.

In a chiral absorber, the impedance matching is polarization dependent. The response to LCP radiation is different from that to RCP radiation. A single scalar impedance does not completely describe this, but the impedance picture still gives a useful interpretation. The proposed configuration seems to be more appropriate for LCP excitation around the main resonance [2] at 25 °C, with nearly unity absorption. RCP excitation does not satisfy the same condition, so absorption is still weaker.

As VO2 becomes more metallic with increasing temperature, both cavity loss and effective impedance change. This changes and lowers the selective resonance condition that preferred LCP at room temperature. This leads to a lower CD value and more Equal absorption between the two circular polarization states.

2.5 Quality Factor and Resonance Selectivity

The quality factor measures the sharpness of a resonance. It is generally written as

$$Q = \frac{\lambda_0}{\Delta\lambda}, \quad 6$$

where λ_0 is the resonance wavelength and $\Delta\lambda$ is the linewidth measured at full width at half maximum. A high-Q resonance is spectrally narrow and sensitive to small perturbations [7]. A lower-Q resonance is broader and less selective.

High Q factor is highly preferred for sensing as small environmental variations are able to cause measurable shifts. For an absorber the interpretation is more neutral. Absorption is not without some loss. If that wasn't enough loss, the energy is stored and then re-radiated rather than dissipated. When the loss is sufficiently high, the resonance becomes broad and weak [4]. The proposed metasurface needs an intermediate condition, where the confinement still is strong, but the energy dissipation is enough.

The VO_2 layer has a direct impact on this balance. In the insulating phase the damping is reduced and the resonant field more localized. In the metallic phase, the small polarization-selective response is weakened and the loss is enhanced by the free carriers. This conclusion is consistent with the observed decrease of CD at 100 °C.

2.6 Fano Resonance and Interference in Metasurfaces

Fano resonance is an asymmetric spectral response that comes from interference between a broad radiative mode and a narrow-localized mode. Such interference in metasurfaces is often due to coupling of bright and dark resonances. The line shape is affected by geometry, loss and symmetry.

The draft which has been provided discusses Fano resonance as the part of theoretical background. In the current metasurface, the spectra exhibit multiple resonance features rather than a single isolated Lorentzian peak. The asymmetric crescent cavities are expected to support different current paths and coupled localized modes [7][2]. A full Fano analysis would require near-field and modal decomposition data, which were not provided.

2.7 Vanadium Dioxide as a Phase-Transition Material

24 Vanadium dioxide is widely studied in tunable photonics because it undergoes a thermally driven insulator-to-metal transition near 68 °C. The transition produces a large change in conductivity and optical response. Wen et al. (2010) used VO_2 cut-wires for thermal tunability in terahertz metamaterials, while Zhang et al. (2019) reported active terahertz control using VO_2-embedded metamaterials. Later work extended VO_2 into metasurface platforms for polarization and modulation control 21 (Tripathi et al. 2021; Li et al. 2022; Zhao et al. 2023).

The advantage of VO_2 in this dissertation lies in its ability to tune the metasurface without changing geometry. Heating changes the active material state. This changes the electric field distribution, induced currents, and damping inside the resonator. The process is especially attractive for compact devices because a thin film is enough to affect the resonance when it is placed in a high-field region.

The present design embeds VO_2 in the resonator cavity. This placement is physically meaningful. If the active film were positioned where the field is weak, the phase transition would have little effect on the spectrum. By locating VO_2 near the cavity

region, the design increases the overlap between the active material and the resonant field.

2.8 Passive and Active Chiral Metasurfaces

A useful way to read the literature is to separate passive chiral metasurfaces from active chiral metasurfaces. Passive structures use fixed geometry and fixed material constants. Their advantage is stability. Once fabricated, the device response is reproducible under the same illumination condition. Their weakness is lack of post-fabrication control. If the resonance wavelength or CD strength is not suitable for the desired task, the design has to be modified and fabricated again.

Active chiral metasurfaces attempt to solve this limitation by adding a material or external control mechanism. Graphene, liquid crystals, GST, and VO_2 appear often in this context. Each material offers a different control route. VO_2 is relevant for the present dissertation because a temperature change produces a large conductivity change [11][13]. This makes it possible to alter the resonance without mechanically moving the structure or changing its geometry.

The choice between passive and active design is not trivial. Active materials introduce extra parameters, and those parameters often bring losses. A passive plasmonic design might show a high CD peak but remain fixed. An active design might offer tuning but lose resonance sharpness [4]. The present work accepts this trade-off and studies it directly. The decrease of CD at 100 °C is not treated as a defect. It is interpreted as the optical signature of active material participation.

2.9 Intrinsic and Extrinsic Chirality

Chirality in planar metasurfaces appears through two routes. We use the intrinsic chirality of the unit cell itself. If the structure lacks mirror symmetry, the opposite circular polarization states couple to different resonant current distributions. Under oblique illumination, extrinsic chirality can emerge if a planar pattern is less chiral or achiral, whereby the structure and the direction of incidence combine to create a handed arrangement.

Intrinsic chirality is therefore expected since the present design is asymmetric Crescent geometry. The angular study also reveals a role of extrinsic effects. At higher angles of incidence, the response of CD increases dramatically [7]. This is an interesting observation because it illustrates that the measured CD depends not only on the shape of the unit cell but also on the way that the electromagnetic wave approaches the structure.

In practical devices, intrinsic chirality is usually preferred, because it allows operation close to normal incidence. In contrast, extrinsic chirality could be used for angular detection or beam-direction sensitive components. The obtained results show that the suggested structure has both features. A more complete study would entail azimuthal-angle sweeps and near-field maps to disentangle the two contributions.

2.10 Why Absorption-Based CD Matters

Circular dichroism is sometimes defined through transmission and sometimes through absorption. The correct definition depends on the device. For a transmissive

chiral polarizer, the difference in transmitted LCP and RCP intensities is the main observable. For a ground-plane absorber, transmission is intentionally blocked. The relevant signal is then the difference in absorption.

Absorption-based CD is useful for detectors and thermal photonic devices [10][6]. If one handedness is absorbed more strongly, the device is able to convert polarization information into heat or electrical signal after integration with a detector layer. The result is not only a polarization filter but also a polarization-sensitive absorber. This is why the present work focuses on A_L and A_R rather than only on reflection or transmission.

The absorption-based definition also makes the role of the ground plane clearer. Since $T \simeq 0$, the device response is largely controlled by reflection. A large value of A_L means that LCP radiation is not transmitted and not reflected significantly at resonance. A low value of A_R at the same wavelength means that RCP radiation fails to couple into the lossy resonant mode. The CD value condenses this contrast into one spectrum.

2.12 Review of Relevant Chiral Metasurface Studies

Several studies in the supplied reference collection frame the present dissertation. Cheng, Chen, and Luo (2021) proposed a bilayer fourfold twisted semicircle metasurface absorber at optical frequency. Their structure achieved high selective absorption for opposite circular polarization states and CD values near 0.85 and 0.91 in different spectral regions. The mechanism was linked to coupling between electric dipole modes in top and bottom layers. This work is relevant because it shows that curved and twisted resonator geometries support strong chiral-selective absorption.

Sharma, Kalra and Sinha (2025) showed a perovskite-based chiral metasurface biosensor that can show CD values in the visible, near-infrared, and mid-infrared bands. Their work connects the design of chiral metasurfaces to practical sensing functions. The present dissertation uses a different active mechanism, but it shares the aim of designing a compact chiral platform with measurable spectral response.

2.13 Position of the Present Work

The proposed metasurface sits between absorber design, chiral polarization control, and VO_2-based active photonics. It is not limited to a passive CD response. It is also not a pure VO_2 switching element. Its contribution lies in combining a chiral hollow crescent resonator with a thermally active VO_2 layer in a ground-plane-backed near-infrared absorber.

The scientific value of this design is best understood through three linked questions. First, does the structure produce high contrast between A_L and A_R? Second, does temperature change this contrast in a measurable way? Third, do geometry and active-layer thickness provide additional design control? The following chapters answer these questions through simulation methodology, result interpretation, and parametric analysis.

CHAPTER 3
PROPOSED METASURFACE DESIGN AND SIMULATION METHODOLOGY

3.1 Design

The proposed metasurface is designed as a compact, thermally tunable, chiral absorber [13]. The structure uses a metal-insulator-metal platform with an active VO_2 layer embedded near the resonant cavity. The bottom gold layer suppresses transmission. The PTFE spacer separates the ground plane from the top resonator and forms the dielectric environment for field confinement. The top gold resonator is made of asymmetric hollow crescent cavities [2], which break the in-plane symmetry and generate different coupling conditions for LCP and RCP excitation.

Absorption requires the incident wave to penetrate the structure and be dissipated. Opposite circular polarization states must excite different current or field distributions for chirality to arise. Tunability requires an external stimulus to change the electromagnetic boundary condition or the material response. The proposed geometry is a combination of these three conditions.

3.2 Unit Cell Geometry

The unit cell has a square periodicity of $p_x = p_y = 600$ nm. The multilayer stack comprises a bottom gold layer, a PTFE dielectric spacer, a thin VO_2 layer, and a top gold resonator. The given draft results in the optimized layer thicknesses of $h_1 = 210$ nm for the bottom gold layer, $h_2 = 160$ nm for the PTFE spacer, $h_3 = 5$ nm for the VO_2 layer, and $h_4 = 40$ nm for the top gold resonator. The crescent widths are denoted by t_1 and t_2 in the design figure.

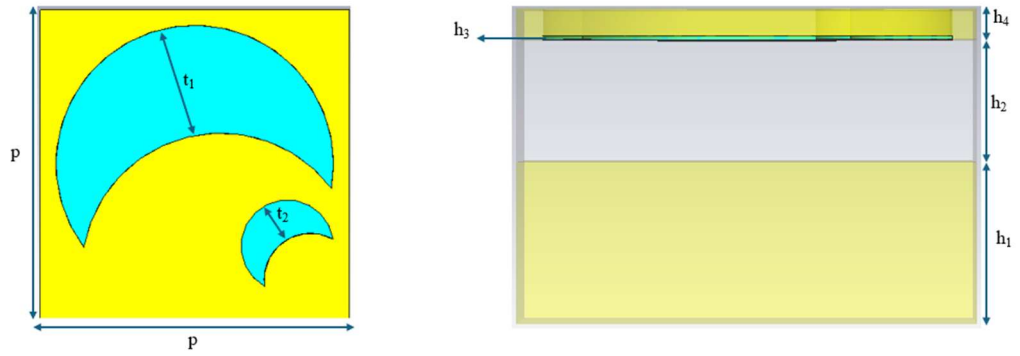

Figure 3.1: Top and side views of the proposed hollow crescent chiral metasurface unit cell.

The top view illustrates two hollow crescent cavities, arranged in an asymmetric manner. This asymmetry is a primary geometrical source of chirality [9]. Under excitation with circularly polarized light, the electric field rotates in time. The nonuniform field concentration [2] by the curved edges of the crescent structure and the fact that the two polarization handedness states do not excite the same current patterns. This results in an unequal absorption of LCP and RCP radiation. The side

view shows that the structure is made up of layers. The bottom gold layer is thick enough to block transmission in the simulated range. The dielectric layer supports the formation of a cavity and separates the resonator from the ground plane. The VO$_2$ layer is positioned at the expected position for a high resonant field [8]. The top gold layer defines the plasmonic resonator and chiral aperture.

Table 3.1: Main structural parameters used for the proposed unit cell.

Parameter	Value	Description
p_x	600 nm	Unit cell periodicity along x direction
p_y	600 nm	Unit cell periodicity along y direction
h_1	210 nm	Bottom gold ground plane thickness
h_2	160 nm	PTFE dielectric layer thickness
h_3	5 nm	VO_2 active layer thickness in optimized design
h_4	40 nm	Top gold resonator thickness
t_1	design parameter	Thickness of first crescent cavity wall
t_2	design parameter	Thickness of second crescent cavity wall

3.3 Material Platform

The top resonator and bottom ground plane are gold. It shows high electrical conductivity and plasmonic response, which makes it ideal for near-infrared resonant structures [9]. In the top layer, gold sustains localized surface currents and field enhancement at the edge. In the bottom layer it inhibits the transmission and stabilizes the absorber's configuration.

The dielectric spacer is made of PTFE. It does not just mechanically separate. It also governs the optical path and field confinement between the resonator and the ground-plane. A low-loss dielectric spacer is important since a strong chiral contrast requires the resonance to be narrow and too much dielectric loss will broaden the resonance.

VO_2 is used as active tunable material. The VO_2 is an insulator or semiconductor with low conductivity at low temperature. At higher temperature it becomes metallic with much larger conductivity [12]. The change in conductivity due to VO_2 phase transition has been employed to control chiral and polarization responses in various metasurface studies (Wen et al. 2010; Zhang et al. 2019; Zhao et al. 2023). This material change changes the local resonant environment inside the crescent cavity in the present structure.3.4 Material Assumptions in Numerical Modelling

Numerical simulation requires material data. Gold, PTFE, and VO_2 must be assigned optical constants or conductivity models in the software. The supplied draft gives the material stack and explains the use of VO_2 as the thermally active layer, while the detailed optical constants used in the CST file were not supplied as raw data. For this reason, the dissertation avoids introducing unsourced numerical optical constants beyond the values explicitly present in the supplied draft and reference collection.

This point matters because VO_2 properties vary with film quality, deposition method, grain structure, and transition history. Reported values in the literature are useful for framing the physics, but a final fabrication-oriented study should state the exact material model used in CST. That includes the complex permittivity or conductivity

assigned to VO_2 at 25 °C and 100 °C, the gold model, and the PTFE dielectric constant. Without these details, the results are best interpreted as a design-level simulation rather than a final manufacturing prediction.

3.4 Reason for Using Two Temperature States

The choice of 25 °C and 100 °C allows a clean comparison between the insulating and metallic states of VO_2. This approach is typical in design-level studies as it separates the two limiting optical responses. Also, the uncertainty in the transition region where the material may have coexisting phases is avoided.

The drawback is that a two-state study does not describe the dynamics of the switch. VO_2 often shows hysteresis, and so the heating and cooling paths can be different. If the device is intended for active operation, then it would be necessary to find out if the CD returns to the original value after repeated cycling. Thus the two-state analysis discussed in this dissertation should be considered as the first evidence of tunability rather than the complete thermal description.

3.5 Circular Polarization Excitation

The simulation needs incident circularly polarised radiation. Circular polarization is represented in a full wave solver by two orthogonal field components with a phase difference of π/2. LCP and RCP differ by the sign of the phase relation. For each incident polarization, the solver calculates the scattering parameters and the corresponding absorption spectrum.

The absorptance values for LCP and RCP excitation are written as

$$A_L(\lambda) = 1 - R_L(\lambda) - T_L(\lambda),$$
$$A_R(\lambda) = 1 - R_R(\lambda) - T_R(\lambda).$$

Because the gold ground plane makes T_L and T_R close to zero, these reduce approximately to

$$A_L(\lambda) \simeq 1 - R_L(\lambda), \qquad A_R(\lambda) \simeq 1 - R_R(\lambda).$$

3.6 Boundary Conditions and Solver Setup

16

The metasurface is periodic in the x and y directions. Periodic boundary conditions are therefore applied along both transverse axes to represent an infinite array. Open boundary conditions are applied along the propagation direction. This configuration is standard for unit cell simulations of periodic metasurfaces.

The supplied draft states that CST Studio Suite was used for full-wave simulation, with the wavelength range selected from 1100 nm to 2500 nm. The frequency-domain finite integration technique solver was used to calculate the electromagnetic response and extract S-parameters. The results were then converted to absorptance and CD spectra.

Table 3.2: Simulation settings used in the supplied study.

Simulation item	Setting
Software	CST Studio Suite
Solver type	Frequency-domain full-wave solver
Wavelength range	1100 nm to 2500 nm
Boundary condition along x	Periodic
Boundary condition along y	Periodic
Boundary condition along z	Open
Incident polarization	LCP and RCP
Output quantities	S_{11}, S_{21}, A_L, A_R, CD
Temperature states	25 °C and 100 °C

3.7 Temperature States

Two temperature states are analysed in the supplied results. The first is 25 °C, where VO_2 is in its low-conductivity state. The second is 100 °C, where VO_2 is treated as being in the high-conductivity metallic state. The two temperatures are selected to characterize the optical response below and above the transition region.

This discrete state approach is enough to demonstrate tunability but doesn't give the complete development of the transition. A continuous temperature sweep would be needed in order to study the hysteresis.

27

CHAPTER 4
RESULTS AND DISCUSSION

4.1 Overview of Temperature-Dependent Response

The optical response of the proposed chiral metasurface was evaluated at 25 °C and 100 °C. These two temperatures represent the low-conductivity and high-conductivity states of VO_2. The purpose of this comparison is to determine whether the phase transition changes the circular dichroism and the polarization-selective absorption of the metasurface.

The results show a clear temperature-dependent change. At 25 °C, the structure exhibits strong circular dichroism, with the supplied draft reporting a peak CD value of 0.829 near 1304 nm. At 100 °C, the peak CD decreases to 0.481 near 1485 nm. The reduction in CD is accompanied by a change in the absorption spectra of LCP and RCP radiation. At low temperature, LCP absorption is much larger than RCP absorption near the main resonance. At elevated temperature, the two absorptance values move closer to each other [4][13].

4.2 Circular Dichroism at 25 °C

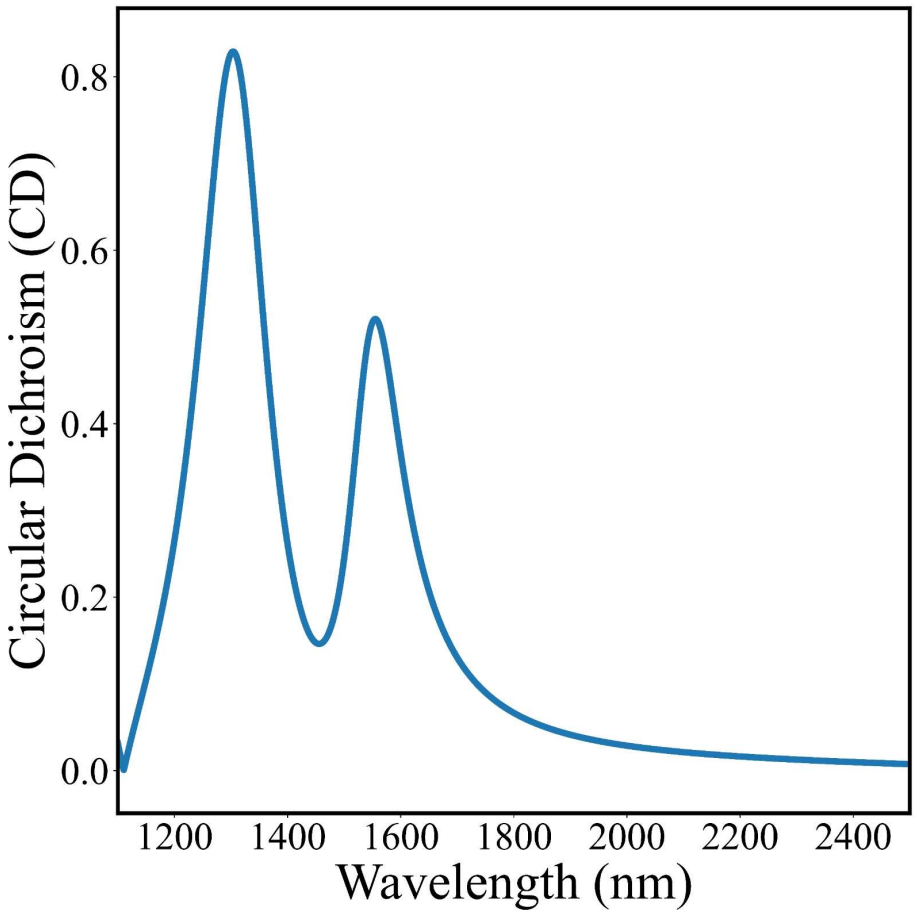

Figure 4.1: Circular dichroism spectrum of the optimized structure at 25 °C.

Figure 4.1 shows the CD spectrum at 25 °C. The strongest peak occurs near 1300 nm. A second smaller peak appears near the mid-range of the spectrum. Beyond about 1800 nm, the CD value decreases gradually and becomes weak in the longer-wavelength region. This spectral profile indicates that the chiral response is resonance-driven rather than broadband.

At 25 °C, VO_2 remains in the low-conductivity state. This state supports stronger confinement inside the resonator cavity. The crescent structure then produces unequal field coupling for LCP and RCP waves. The high CD peak suggests that one circular polarization state excites a strong localized mode [2], while the other excites a weaker mode or couples less efficiently to the absorbing region.

4.3 Polarization-Dependent Absorption at 25 °C

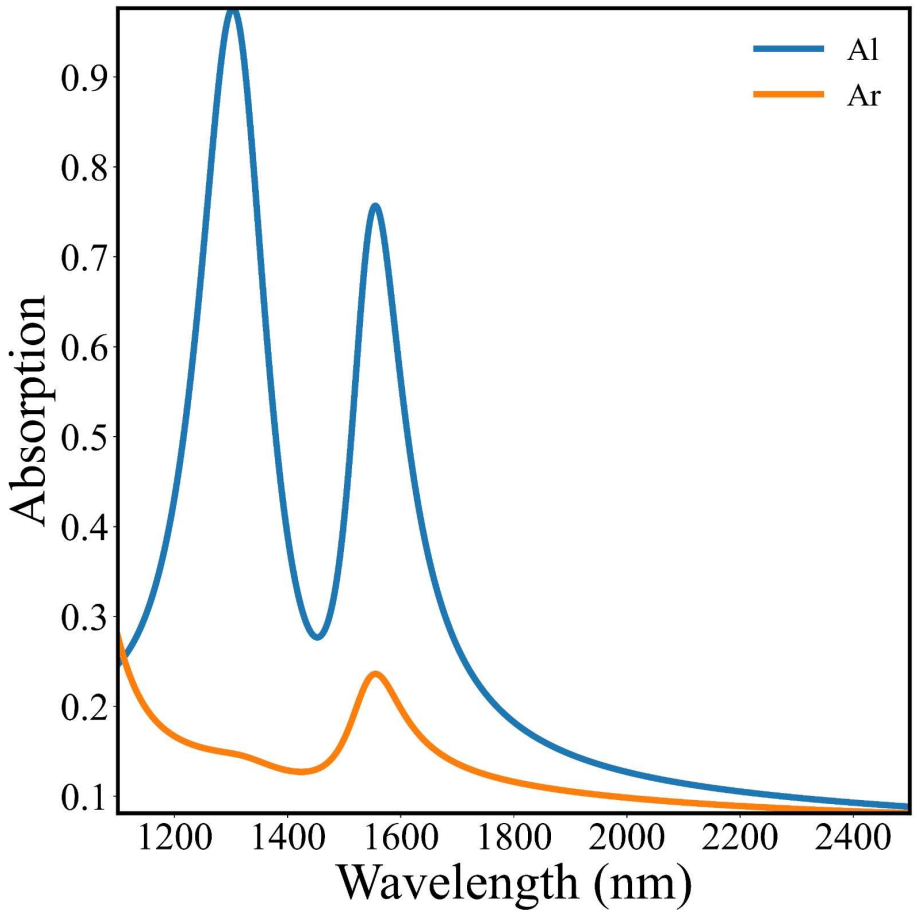

Figure 4.2: Absorption for LCP and RCP radiation at 25 °C for the optimized geometry of metasurface

Figure 4.2 shows A_L and A_R at 25 °C. The supplied draft reports $A_L = 0.976$ and $A_R = 0.275$ near the main resonance. This large difference is the direct origin of the high CD value. The result means that the structure absorbs left circularly polarized radiation strongly, while right circularly polarized radiation is much less absorbed at the same spectral region.

The near-unity value of A_L suggests effective resonance confinement and reflection suppression for the LCP state. Since the ground plane already suppresses transmission, high absorption requires low reflection [2]. The structure appears to approach this condition for LCP excitation [2]. RCP excitation does not satisfy the same condition, so a larger part of the incident energy is reflected or weakly coupled.

This result also confirms that the observed CD is not a numerical artifact caused by a small difference between two weak absorption signals. It is based on a large contrast between one strong absorption channel and one weaker absorption channel. The physical interpretation is that the asymmetric crescent cavity creates a handed near-field environment. The rotating electric field of LCP radiation aligns with the resonant current pathway more efficiently than RCP radiation near the main peak.

4.4 Circular Dichroism at 100 °C

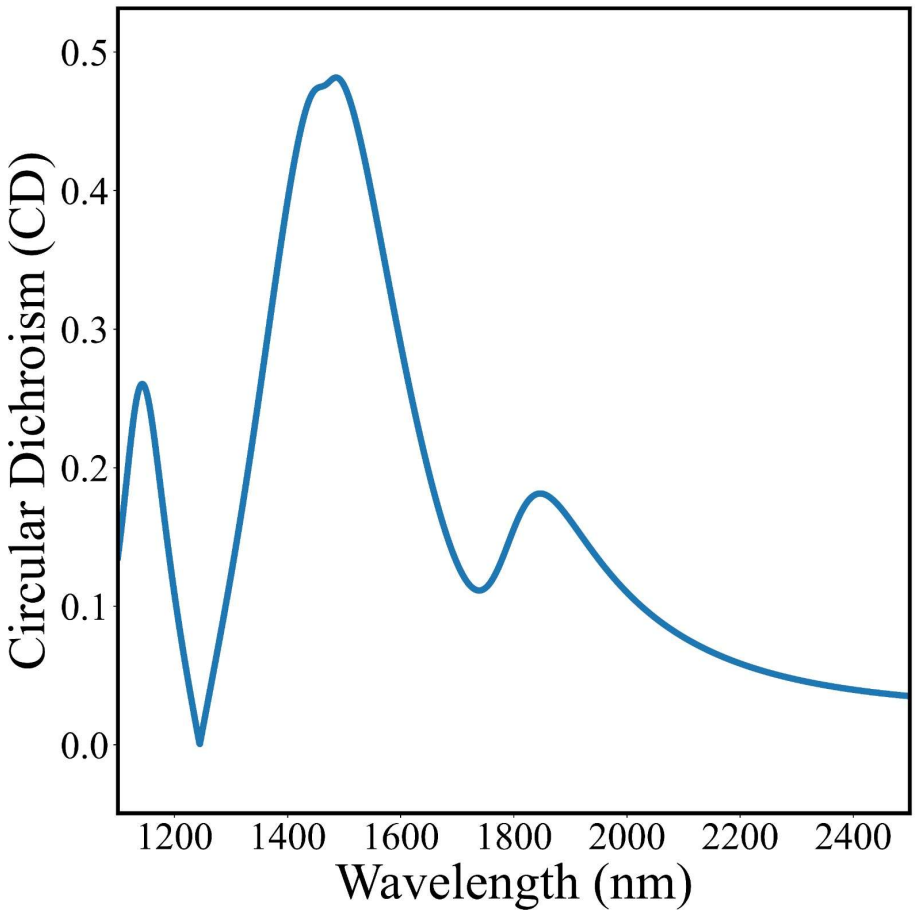

Figure 4.3: Circular dichroism spectrum of the optimized structure at 100 °C

Figure 4.3 shows the CD response at 100 °C. The main peak shifts toward a longer wavelength and becomes lower than the room-temperature peak [13]. The supplied draft reports a peak CD of 0.481 near 1485 nm. This reduction suggests that the metallic phase of VO_2 weakens the chiral selectivity of the cavity.

The change is physically plausible. The metallic phase of VO2 shows an increased free-carrier concentration that modifies the local optical constants. In the insulating

state the cavity cannot sustain the same field distribution . Larger damping results in a broader response and a reduction of the difference between the LCP and RCP absorption. The resonance is still present, so the structure is not optically inactive at 100 °C. Instead, it enters a different state with reduced polarization discrimination.

4.5 Polarization-Dependent Absorption at 100 °C

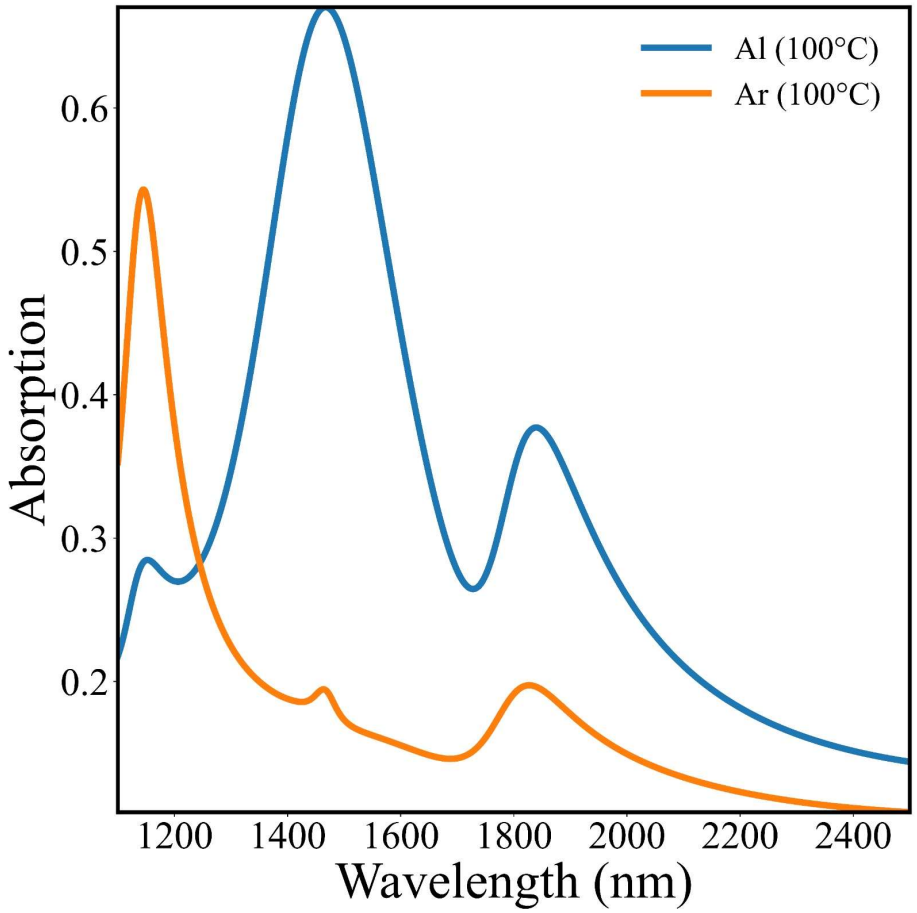

Figure 4.4: Absorption spectra for LCP and RCP radiation at 100 °C

Figure 4.4 shows the absorption spectra at elevated temperature. The supplied draft reports $A_R = 0.543$ and $A_L = 0.670$ near the resonance used for comparison. The difference between the two polarization channels is smaller than at 25 °C. The CD value therefore decreases.

This result indicates that the metallic VO_2 phase redistributes the resonant response [12]. RCP absorption increases relative to its room-temperature value, while LCP absorption decreases from the near-unity value observed at 25 °C. The high-temperature state therefore does not simply reduce absorption everywhere. Instead, it changes the balance between the two handed channels.

The underlying reason is likely a combination of three effects. First, the conductivity increase changes current flow inside the VO_2 region. Second, additional damping weakens the sharp LCP-selective resonance [4]. Third, the effective impedance

condition moves away from the low-reflection state for LCP and becomes less asymmetric between polarizations. The net result is a smaller CD value.

4.6 Reading the Two-Peak CD Profile

The room-temperature CD spectrum contains a dominant peak near 1300 nm and a smaller peak at longer wavelength. The presence of more than one feature indicates that the crescent unit cell is supporting multiple resonant pathways [7]. They may arise from different regions of the curved cavity, coupling between the top resonator and ground plane [2].

The high temperature CD spectrum exhibits several features but the relative shape is altered. This means VO_2 does not affect all modes equally. Modes with larger field overlap in the VO2 region should be more sensitive to the phase transition . Future near-field analysis should compare the field intensity inside the VO_2 layer at each resonance wavelength..

4.7 Modulation Depth of Circular Dichroism

The change in CD can be described with the help of a simple modulation depth. Using the reported peak values,

$$M_{\mathrm{CD}} = \frac{\mathrm{CD}_{25} - \mathrm{CD}_{100}}{\mathrm{CD}_{25}} \times 100\%. \qquad 6$$

Substitution of $\mathrm{CD}_{25} = 0.829$ and $\mathrm{CD}_{100} = 0.481$ gives approximately 42 percent. This value illustrates the fractional reduction of the peak value of CD between the two temperature states namely 25℃ and 100℃ .

The two peaks are at different wavelengths. A device designer might instead compare CD at a particular wavelength since a detector or modulator is often designed to operate at one wavelength. The data presented exhibit both spectral and amplitude modulation.4.10 Quantitative Comparison Between Temperature States

Table 4.1: Key simulated chiroptical results at 25 °C and 100 °C.

Temperature	Peak CD	Resonance wavelength	A_L	A_R
25 °C	0.829	1304 nm	0.976	0.275
100 °C	0.481	1485 nm	0.670	0.543

Table 4.1 illustrates the main results. The value of CD decreases from 0.829 to 0.481 when the temperature increases from 25 °C to 100 °C. The resonance wavelength also shifts from 1304 nm to 1485 nm.

4.8 Physical Interpretation of the Temperature Response

The temperature response observed is due to the phase transition of VO$_{2}$. The phase with a low conductivity supports a strong localized resonance in the cavity at 25 °C. The asymmetric crescent shape leads to a different coupling to LCP and RCP radiation. The LCP excitation approaches better the resonant condition leading to a large absorption peak and high CD.

At 100 °C the VO2 layer is more metallic. This modifies the effective permittivity and increases the conductivity. Thus, the current paths and the field confinement within the cavity are changed [12]. A metallic active layer also increases the ohmic damping which reduces the sharpness and selectivity of the resonance. The LCP dominant absorption channel is suppressed and the RCP absorption is enhanced. Then the structure has a smaller difference between Al and AR.Studies on VO_2-based tunable metasurfaces report that the phase transition changes transmission, reflection, absorption, and polarization response by altering conductivity and resonant coupling (Wen et al. 2010; Zhang et al. 2019; Zhao et al. 2023). The present work extends the same principle to a near-infrared chiral absorber based on hollow crescent resonators.

4.9 Comparison With Reported Metasurface Studies

Table 4.2: Comparison with selected studies from the supplied reference collection.

Study	Structure or platform	Reported response	Relevance to this work
Landy et al. (2008)	Metal-based metamaterial absorber	Simulated absorption near 96 percent and experimental peak above 88 percent	Establishes absorber physics through reflection and transmission suppression
Cheng, Chen, and Luo (2021)	Bilayer twisted semicircle chiral absorber	Selective absorption above 90 percent and high CD	Shows strong CD from curved chiral resonators
Zhao et al. (2023)	VO_2-based chiral metasurface	AT 0.95 and CCD 0.92 with thermal switching	Demonstrates VO_2-driven active chiral control
Sharma, Kalra, and Sinha (2025)	Perovskite chiral metasurface biosensor	CD in visible, NIR, and MIR bands with sensing applications	Links CD response to multifunctional sensing
Present work	Gold-PTFE-VO_2 hollow crescent absorber	CD 0.829 at 25 °C and 0.481 at 100 °C	Studies near-infrared thermal tuning of absorption-based CD

The comparison in Table 4.2 shows that the present work fits within an active and absorption-based metasurface research direction. Its peak CD is comparable to strong chiral absorber studies, although the purpose is not only to maximize CD. The central result is the reduction and spectral shift of CD after thermal activation of VO_2.

A further distinction lies in the operating mechanism. Zhao et al. (2023) focused on asymmetric transmission and circular conversion dichroism in a VO_2-based structure. The present work focuses on differential absorption in a ground-plane-backed near-infrared structure. This difference matters because absorber-based devices are often more relevant for detectors, thermal emitters, sensing platforms [6], and compact modulators.

CHAPTER 5
PARAMETRIC ANALYSIS

5.1 Purpose of Parametric Evaluation

A metasurface response depends strongly on geometry and material placement. Parametric analysis is therefore necessary for understanding how the design behaves when a key structural variable changes. In this dissertation, two parameters are emphasized: VO_2 layer thickness and angle of incidence. The VO_2 thickness controls the interaction volume of the active material [8]. The incidence angle modifies the projection of the incident field on the asymmetric resonator geometry.

5.2 Effect of VO_2 Layer Thickness

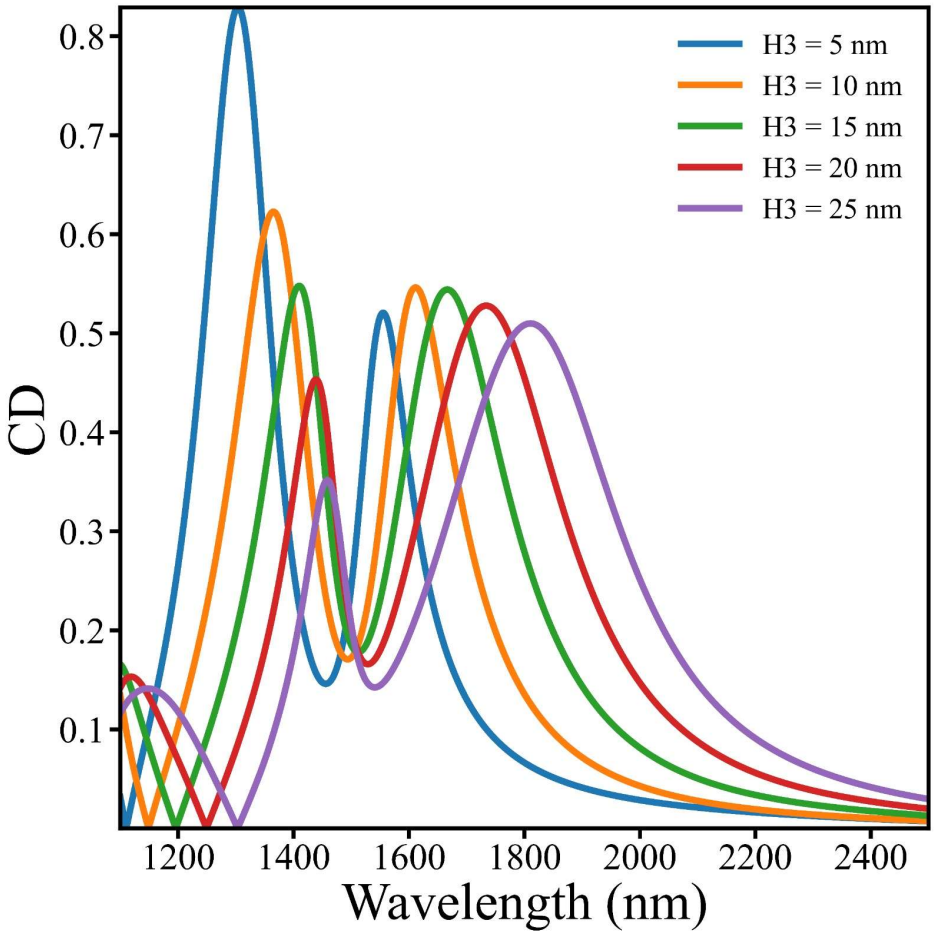

Figure 5.1: CD vs Wavelength at 25 °C for different VO_2 layer thicknesses h_3

Figure 5.1 shows the CD vs Wavelength curve variation with thickness of VO_2 from 5 nm to 25 nm respectively. The strongest and sharpest main resonance in the plotted response is observed for the 5 nm case. For increasing VO_2 thickness the dominant resonance is shifted to longer wavelengths and broadened. The magnitude at the peak also varies.

This trend indicates the effect of the VO_2 layer on the effective refractive index and loss inside the cavity. Increasing the thickness of the VO_2 layer increases the fraction of resonant mode overlapping with the active material. This increases the optical interaction with VO_2, but also damping [4]. If the damping is too large, the polarization selective confinement is weakened and the CD peak is decreased or broadened.

The red shift with increasing thickness is consistent with an increased effective optical pathlength. In a resonant cavity , higher effective refractive index or larger optical thickness shifts the resonance to longer wavelength.

The data provided seems to give the best balance with the 5 nm case. It is thin enough not to damp excessively but placed in a region where the resonant field is strong enough for temperature tuning. This is why the optimized design with h_3 =5nm is used.

5.3 Interpretation Through Loss and Field Overlap

The thickness dependence reflects a competition between field overlap and resonant quality. If the VO_2 film is too thin, the active layer might not strongly tune the response. If it is too thick, the resonance is likely to suffer increased damping. The supplied graph indicates that the second effect becomes important as thickness increases beyond the optimized value.

This result aligns with the broader literature on active metasurfaces. Phase-change materials are most effective when placed in regions of high field concentration [8]. Yet active materials also introduce loss [4], especially in metallic or intermediate states. A good design therefore uses a small volume of active material at a strategically important location.

Table 5.1: Qualitative effect of increasing VO_2 thickness based on the supplied CD spectra.

Observed change	Physical interpretation
Main peak shifts toward longer wavelength	Increased effective optical path and altered cavity phase
Peak broadening [4]	Stronger damping and reduced resonance quality
Reduced sharpness at larger thickness	Weaker polarization-selective confinement
Stronger response at 5 nm	Better balance between active tuning and controlled loss

5.4 Design Guidelines From the Thickness Study

The thickness study suggests several design guidelines. A thin VO_2 layer placed at a high-field region is likely to be more effective than a thicker layer distributed through a larger volume [8]. The 5 nm optimized case supports this interpretation. It gives strong CD while preserving a sharp main resonance.

Increasing the VO_2 thickness shifts the resonance and broadens the spectrum. This does not mean thicker VO_2 is always undesirable. If the goal is broadband absorption or stronger thermal contrast at a different wavelength, a thicker layer might be useful. If the goal is high peak CD at the original resonance, the thinner layer appears better.

The design choice should therefore be tied to the intended device. A narrowband sensor benefits from sharp resonance. A thermal modulator might benefit from stronger spectral movement. A broadband absorber might accept reduced peak CD in exchange for wider response. The present dissertation uses the high-CD design as the main optimized case.

5.5 Thickness and Temperature Coupling

The supplied thickness study is performed at 25 °C. A more complete analysis would repeat the thickness sweep at 100 °C and possibly at intermediate temperatures. This would show whether the optimal thickness for high room-temperature CD is also optimal for thermal modulation depth.

It is possible that a thickness larger than 5 nm might produce a lower CD at 25 °C but a larger difference between temperature states. If the target is switching rather than maximum low-temperature CD, the optimum might change. This is another reason to treat design optimization as application-specific.

5.6 Angular Dependence of the Chiral Response

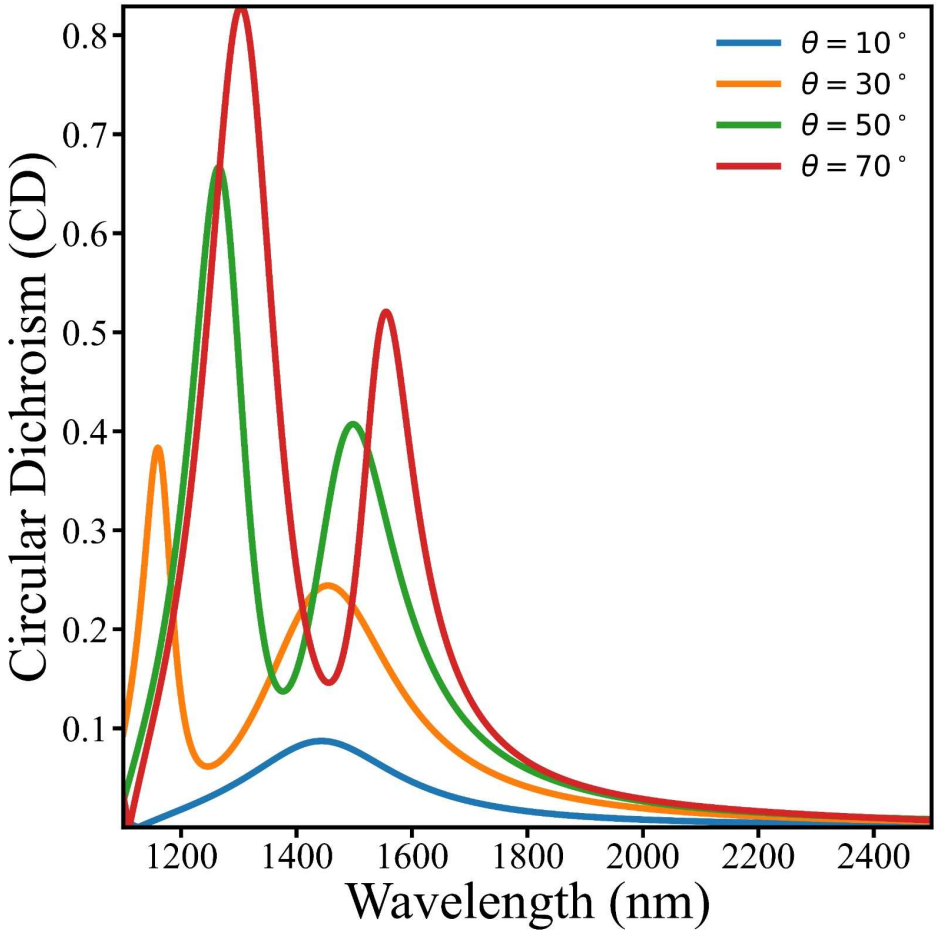

Figure 5.2: Circular dichroism spectra at 25 °C for different incidence angles.

Figure 5.2 shows CD spectra for incidence angles of 10°, 30°, 50°, and 70°. The response changes strongly with angle [7]. At 10°, the CD response is close to 0.1. At higher angles, the CD values start to increase, with the 70° curve having a CD response of 0.82

25 This result implies an extrinsic contribution to chirality. Intrinsic chirality arises from the asymmetric geometry of the unit cell itself. Extrinsic chirality arises when the direction of incidence and the planar structure combine to generate a handed arrangement. The electric and magnetic field components interact with the resonator for oblique incidence differently than for near-normal incidence. This alters the distribution of induced current and the CD response.

5.7 Angular Response and Practical Design

The angular response has two implications. First, the structure offers a way to tune CD through illumination geometry. Second, it highlights a design trade-off. A metasurface designed for maximum CD at oblique incidence might perform weakly at normal incidence. A device designed for broad angular stability might need a more symmetric or multilayer compensation strategy.

For practical infrared sensing, the incident beam is rarely perfectly normal across the full device area. Angular robustness is therefore important. Future work should test intermediate angles, both azimuthal and polar, and evaluate the response under finite numerical aperture illumination. The supplied results only cover a selected angular sweep, but they are enough to show that incidence angle is a major control variable.

CHAPTER 6
PHYSICS-BASED DISCUSSION AND DESIGN IMPLICATIONS

6.1 Role of the Hollow Crescent Geometry

The core of the proposed design is the hollow crescent geometry of the metasurface.The two crescent cavities are not arranged in a mirror symmetric way and therefore the response for rotating fields with opposite handedness is different.

A simple straight resonator could support strong absorption, but not necessarily strong CD. The crescent shape imparts a rotary character to the current path. The coupling is stronger for the case where the circularly polarized field rotates in the same effective sense as the resonant current pathway.

6.2 Role of the Gold Ground Plane

The ground plane changes the device from a transmissive metasurface to absorber. Without the ground plane incident energy would be split between reflection, transmission and absorption. The ground plane reduces the transmission. The design problem then is to provide for reflection control and dissipation.

That is why the absorption relation simplifies to A~1-R. If the absorption peak is high then the structure does not reflect a lot of that wavelength energy. In the present design the ground plane has image currents also coupled to the top resonator.

6.3 Role of PTFE Dielectric Spacer

The PTFE layer is a dielectric layer that separates the top resonator from the ground plane and defines the cavity region. It also has an impact on electric and magnetic coupling strength that occurs between top resonator and bottom metal layer.

If the spacer is too thin, there will be strong near-field coupling, but this may increase loss and reduce tunability. A spacer that is too thick would reduce the resonator-ground-plane interaction. The provided optimized value of 160 nm is a design choice to support near-infrared resonant absorption in the range of simulation.

6.4 Role of VO_2 Placement

Placement of the VO2 in the resonator cavity is an important design choice. The active material should be on top of the localized field. Otherwise, its phase transition would have only a weak effect on the spectral response.

At room temperature the thin VO_2 film retains the chiral resonance sharp enough to realize large polarization contrast. At high temperature the same layer modifies the resonance by an increase of conductivity. Thus, the position of VO_2 determines both the baseline response and the tunable shift.

6.5 Why Circular Dichroism Falls at High Temperature

The loss of the CD at 100 °C does not occur because of geometry of the proposed metasurface. This is the signal that it is actively tuning itself. The metallic phase of VO$_2$ enhances the damping and changes the current distribution. The resonance preferred by the LCP at 25°C is no longer selective. RCP absorption increases and LCP absorption decreases. Therefore, CD, which is the difference of the two, becomes smaller.

6.6 Limitations of the Present Study

Present work is simulation based. This is a necessary first step, but leaves many questions unanswered. Real VO_2 films exhibit hysteresis, grain dependence, and fabrication-dependent optical constants. These effects were absent in the supplied data. The temperature analysis uses two states rather than a continuous sweep. It establishes tunability but does not define switching threshold, hysteresis loop, or modulation depth across intermediate temperatures. Future work should include these aspects.

6.7 Scientific Contribution

20

The main contribution of this dissertation is the design and analysis of a VO_2-integrated hollow crescent chiral metasurface absorber that exhibits strong near-infrared CD at room temperature and a reduced, shifted CD response at high temperature. The work combines an absorption-based chiral geometry with an active phase-transition layer and interprets the result through resonance confinement, impedance matching, and conductivity-induced damping.

The dissertation also provides a structured comparison with related chiral metasurface studies. It shows that the proposed design is part of a broader movement from passive metasurfaces toward active, reconfigurable photonic devices. Its most useful result is not only a single high CD value, but the demonstration that the CD response changes substantially when VO_2 crosses into the metallic state.

CHAPTER 7
CONCLUSION, FUTURE SCOPE AND SOCIAL IMPACT

7.1 Conclusion

This dissertation presented the design and simulation-based analysis of a temperature tunable chiral metasurface operating in the near-infrared region. The proposed structure uses a multilayer gold-PTFE-VO_2-gold configuration with an asymmetric hollow crescent top resonator. The device was analysed using CST Studio Suite over the wavelength range of 1100 nm to 2500 nm in the near infrared region.

At 25 °C, the structure shows strong polarization-selective absorption of the light. The supplied results report a peak CD of 0.829 near 1304 nm, with $A_L = 0.976$ and $A_R = 0.275$. This shows that at low-temperature VO_2 supports strong asymmetric coupling that takes place inside the chiral resonator cavity. The high LCP absorption shows effective impedance matching and resonance confinement for one handedness of circular polarization.At 100 °C, the CD decreases to 0.481 near 1485 nm. The absorption contrast between LCP and RCP radiation becomes smaller, with values of $A_L = 0.670$ and $A_R = 0.543$ reported in the supplied draft. This change is attributed to the insulator-to-metal transition of VO_2. The high-conductivity phase modifies the cavity response, increases damping, and weakens the polarization-selective resonance. In addition, the parametric study shows the strong effect of the VO2 thickness and incidence angle on the CD spectrum. The thickness cases presented show the strongest response for a 5-nm VO_2 layer. Resonance shifts and broadens at larger thicknesses. The angular study shows that the CD response is enhanced in the plotted range for oblique incidence which is a signature of the incidence induced chirality contribution.

In brief, the results are consistent with the main argument of the thesis, namely a VO 2 -assisted hollow crescent chiral metasurface provides a practical approach for thermally tunable circular dichroism and polarization-selective absorption in the near-infrared region.

7.2 Major Findings

The main findings are listed below.

1. The proposed chiral metasurface illustrates a strong CD value of 0.829 at 25 °C near 1304 nm.
2. When the temperature is 100 °C the value of CD reduces to 0.481 near 1485 nm.
3. The resonance is tuned by the VO2 phase transition by conductivity, effective permittivity, damping and impedance conditions.
4. The thickness of VO_2 layer affects the magnitude of CD as well as spectral position.
5. Incidence angle impacts the magnitude of CD and the absorption of LCP and RCP respectively.

7.3 Future Scope

The present work leads to several directions. The first step is to perform a continuous temperature scan. Simulations at 25°C and 100°C show two end states but do not show the evolution of CD through the transition region. A temperature sweep from room temperature to greater than 100℃ would be valuable to quantify the switching contrast, transition slope, and intermediate optical states.

Secondly, the full geometry shall be optimized along with the other parameters. The thickness of the crescent, the radius of the cavity, the spacing of the gaps and the orientation of the resonator have to be changed systematically. Such optimization can improve the peak CD value or improve the angular stability [7].

Third, the CST software shall be used to extract the near field distributions. as these distributions would improve the physical interpretation of the resonance. This would directly indicate which parts of the crescent cavity contribute most to the LCP and RCP responses.

7.4 Possible Applications

The proposed structure has significance across multiple application areas. It may serve as a tunable polarization-selective absorber for infrared photonics. In sensing, CD changes could be used to discriminate changes of the temperature, refractive index or the molecular chirality [10][6]. A temperature-responsive, polarization selective absorber could be used for adaptive filtering in thermal imaging. All these applications could be implemented.

7.5 Final Remarks

The dissertation demonstrates that material tunability and structural chirality are not independent design problems.

The polarization selectivity is generated by the hollow crescent geometry and the resonance state is tuned by temperature through VO$_2$. The central result of the study is the CD modulation obtained. The work's strongest point is its clear physical progression: artificial electromagnetic design, chiral resonance formation, absorption control and active thermal tuning.

APPENDIX-A
SUPPLEMENTARY SIMULATION RELATIONS

A.1 Absorption From Scattering Parameters

The absorptance relation used in the research work follows from the [principle of conservation of energy [2]. For each circular polarization state, we have

$$A_{L,R}(\lambda) = 1 - \left|S_{11,L,R}(\lambda)\right|^2 - \left|S_{21,L,R}(\lambda)\right|^2.$$

For a gold-backed metasurface, $|S_{21}|^2$ is close to zero, so

$$A_{L,R}(\lambda) \simeq 1 - \left|S_{11,L,R}(\lambda)\right|^2.$$

The circular dichroism is given as

$$\mathrm{CD}(\lambda) = A_L(\lambda) - A_R(\lambda).$$

REFERENCES

1. Barron, L. D. 2009. *Molecular Light Scattering and Optical Activity*. Cambridge: Cambridge University Press.
2. Cheng, Yongzhi, Fu Chen, and Hui Luo. 2021. "Plasmonic Chiral Metasurface Absorber Based on Bilayer Fourfold Twisted Semicircle Nanostructure at Optical Frequency." *Nanoscale Research Letters* 16: 12. https://doi.org/10.1186/s11671-021-03474-6.
3. Landy, N. I., S. Sajuyigbe, J. J. Mock, D. R. Smith, and W. J. Padilla. 2008. "Perfect Metamaterial Absorber." *Physical Review Letters* 100: 207402. https://doi.org/10.1103/PhysRevLett.100.207402.
4. Li, B., R. Camacho-Morales, N. Li, A. Tognazzi, M. Gandolfi, D. de Ceglia, C. De Angelis, A. A. Sukhorukov, and D. N. Neshev. 2022. "Fundamental Limits for Transmission Modulation in VO_2 Metasurfaces." *Photonics Research* 11: B40-49. https://doi.org/10.1364/PRJ.476487.
5. Pendry, J. B. 2004. "Negative Refraction." *Contemporary Physics* 45: 191-202. https://doi.org/10.1080/00107510410001667434.
6. Sharma, Vishakha, Yogita Kalra, and Ravindra Kumar Sinha. 2025. "Triple-Band Perovskite Based Chiral Metasurface Biosensor with Multi-Functionalities." *Journal of Computational Electronics* 24: 97. https://doi.org/10.1007/s10825-025-02332-3.
7. Shi, T., Z.-L. Deng, G. Geng, X. Zeng, Y. Zeng, G. Hu, A. Overvig, et al. 2022. "Planar Chiral Metasurfaces with Maximal and Tunable Chiroptical Response Driven by Bound States in the Continuum." *Nature Communications* 13: 4111. https://doi.org/10.1038/s41467-022-31714-1.
8. Tripathi, A., J. John, S. Kruk, Z. Zhang, H. S. Nguyen, L. Berguiga, P. R. Romeo, et al. 2021. "Tunable Mie-Resonant Dielectric Metasurfaces Based on VO_2 Phase-Transition Materials." *ACS Photonics* 8: 1206-13. https://doi.org/10.1021/acsphotonics.0c01955.
9. Valev, V. K., J. J. Baumberg, C. Sibilia, and T. Verbiest. 2013. "Chirality and Chiroptical Effects in Plasmonic Nanostructures: Fundamentals, Recent Progress, and Outlook." *Advanced Materials* 25: 2517-34. https://doi.org/10.1002/adma.201205178.
10. Warning, L. A., A. R. Miandashti, L. A. McCarthy, Q. Zhang, C. F. Landes, and S. Link. 2021. "Nanophotonic Approaches for Chirality Sensing." *ACS Nano* 15: 15538-66. https://doi.org/10.1021/acsnano.1c05036.
11. Wen, Q. Y., H. W. Zhang, Q. H. Yang, Y. S. Xie, K. Chen, and Y. L. Liu. 2010. "Terahertz Metamaterials with VO_2 Cut-Wires for Thermal Tunability." *Applied Physics Letters* 97: 021111. https://doi.org/10.1063/1.3463466.
12. Zhang, C., G. Zhou, J. Wu, Y. Tang, Q. Wen, S. Li, J. Han, B. Jin, J. Chen, and P. Wu. 2019. "Active Control of Terahertz Waves Using Vanadium-Dioxide-Embedded Metamaterials." *Physical Review Applied* 11: 054016. https://doi.org/10.1103/PhysRevApplied.11.054016.
13. Zhao, Songliang, Huan Jiang, Jingyu Wang, Wenchang Zhu, and Weiren Zhao. 2023. "Large-Range Switchable Asymmetric Transmission and Circular Conversion

Dichroism in a VO_2 Based Metasurface." *Photonics* 10 (8): 893. https://doi.org/10.3390/photonics10080893.